

# Embedded Sensors for Biomimetic Robotics via Shape Deposition Manufacturing

Aaron M. Dollar, Christopher R. Wagner, and Robert D. Howe

*Division of Engineering and Applied Sciences  
Harvard University  
Cambridge, MA 0138, USA  
adollar@deas.harvard.edu*

**Abstract** –One of the greatest successes of biologically-inspired design has been the development of mechanically robust robots. One promising biomimetic fabrication technique is shape deposition manufacturing (SDM), which alternates material deposition and machining to produce robot structures with compliant joints and embedded actuation elements. In this paper, we add to the tools available to robot designers by describing the development of a range of sensing modalities. These include Hall-effect sensors for joint angle sensing, embedded strain gauges for 3 axis force measurements, optical reflectance sensors for tactile sensing, and piezoelectric polymers for contact detection. We demonstrate these sensors in the context of a simple robotic grasper using the biomimetic SDM process to simplify fabrication and produce robust sensing mechanisms.

**Index Terms** – Embedded Sensors, Tactile Sensing, Robot Design, Shape Deposition Manufacturing, Rapid Prototyping.

## I. INTRODUCTION

One of the most intriguing successes in biomimetic robot design is the Sprawl family of robots (Fig. 1) [1]. Named after the sprawled leg configuration of many arthropods, these robots mimic the design and control of the cockroach, chosen because of its well-studied locomotion dynamics and robust performance characteristics. One of the most notable features of the Sprawl robots is that the hip joint is a passive rubber spring connecting the legs to the body. This joint, mimicking the springy, resilin lined joints of the insect [2], aids in disturbance rejection, accomplished without sensory feedback. The robots have shown robust performance in extremely rugged terrain while operating in a purely feed-forward manner.

A foundational premise of the Sprawl robot project was that traditional components and manufacturing techniques are not well-suited for the construction of biomimetic structures. Instead, a new manufacturing process called Shape Deposition Manufacturing (SDM) [3] was expanded upon for application to robotics [1]. The modified process

uses polymeric materials to simultaneously create the rigid links and compliant joints, with embedded sensing and actuation components. Elastomeric polymers provide joint compliance, eliminating metal bearings, and tough rigid polymers fully encase the embedded components, eliminating the need for seams and fasteners that are often the source of mechanical failure.

In addition to simplifying the construction process, SDM produces extremely robust components. Although not created using SDM, examples of durable robots for industrial, space, and military applications include iRobot's "PackBot" [4], University of Minnesota's "Scout" family of launchable robots [5], and MIT manipulator arms for the NASA/JPL Pathfinder and Surveyor Mars missions [6]. In research, this durability would expand the type of experimental tasks that can be reasonably attempted and speed implementation due to the reduced need for careful validation of programs. This robustness is a key attribute of animals and has substantial benefits for robots.

While they have demonstrated good performance and shown great promise for future work, the Sprawl robots and other robot mechanisms built using the SDM process have been purely passive or open-loop mechanisms, devoid of sensing and control [7, 8]. In order to expand the usefulness of SDM, sensors must be developed that both integrate with and exploit the unique characteristics of the process.

In this study, we describe the development of four types of sensors that take advantage of the special properties of the SDM process: an angular sensor for flexural joints, a force sensor with embedded strain gages, a compliant tactile sensor, and a low-threshold contact sensor. While they are broadly useful in many robotic applications, we evaluate these sensors in robotic graspers. Results show that SDM can bring the benefits of robustness and simplified construction to a wide variety of robotic sensing applications.

## II. SHAPE DEPOSITION MANUFACTURING

Shape Deposition Manufacturing (SDM) is a rapid prototyping process involving a cycle of deposition of part material and shaping that builds up the part in distinct layers, resulting in the concurrent manufacture and assembly of the part. In this way, the part can be

---

\* This work was supported in part by the Office of Naval Research grant number N00014-98-1-0669.

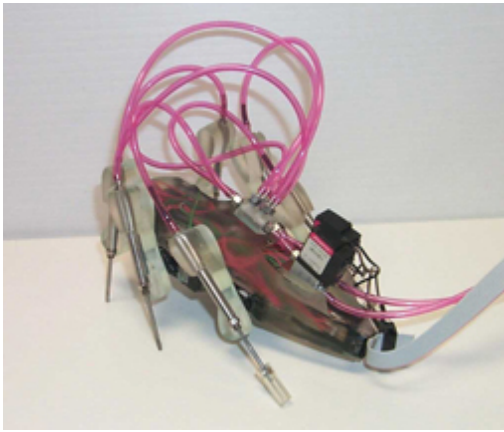


Fig. 1 Sprawlita. Courtesy of Mark Cutkosky.

TABLE I  
MATERIALS SPECIFICATIONS

	IE20AH	IE35A	IE90A	IE72DC
Hardness	15-25A	30-40A	85-95A	75-85D
Tensile Strength ASTM D-638 (ksi)	0.2	0.4	1.8	10
Elongation at Break	175%	470%	100	2%
Tear Strength ASTM D-624 (pil)	25	50	250	N/A
Flex Modulus ASTM D-790 (ksi)	N/A	N/A	N/A	325
Ultimate Flex Strength D-790 (ksi)	N/A	N/A	N/A	13

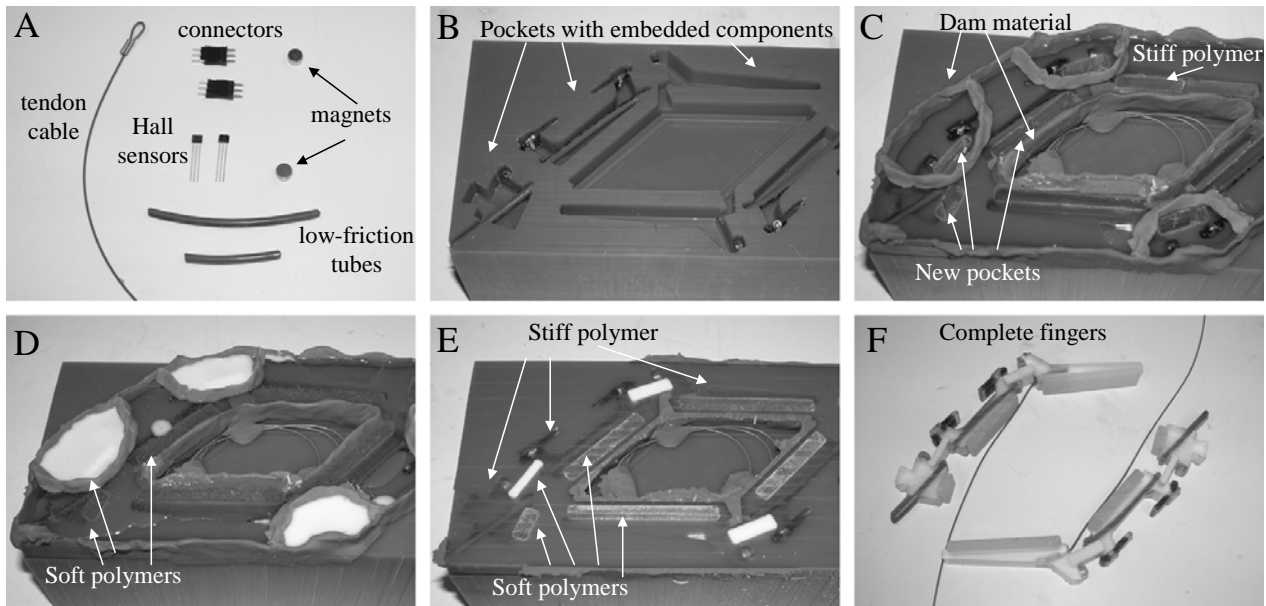


Fig. 2 Steps of the Shape Deposition Manufacturing (SDM) process used to fabricate the grasper fingers.

manufactured in multiple sections or layers, allowing manipulation of the internal parts of the structure. A detailed example use of the process is given in the next section.

This process has a number of advantages over other prototyping techniques. The deposition of part material allows components to be embedded into the part during production, eliminating the need for fasteners, and reducing the likelihood of damage to the component by encasing it within the part structure. This is a particularly desirable property for the inclusion of fragile components such as sensors, greatly increasing the robustness of the part. Also, depositing the part in layers permits the use of dissimilar materials, allowing for variation of mechanical properties within the same part. This property can be utilized to create complex one-part mechanisms using common computer numerical controlled (CNC) mill machines [1, 7-9].

#### Grasper Design and Fabrication

In previous work, we examined the optimization of the design of simple four-joint, two-fingered grippers with passive springs in the joints [10]. These studies showed that for a particular set of joint stiffnesses and rest angles, objects could be securely grasped for the widest range of uncertainty in object size and location. Contact forces were also minimized at approximately the same gripper configuration. Based on this optimum design, we constructed an SDM gripper to enable further investigation into grasping in unstructured environments. This gripper currently lacks much of the sensing necessary to allow for complex manipulation tasks. The sensors described in this paper will be integrated into this design to extend its capabilities.

The diagram in Fig. 2 shows the steps of the SDM process used to produce our compliant grasper fingers. Pockets corresponding to the shape of the stiff links of our fingers are machined into a high-grade machine wax (Freeman Manufacturing and Supply Co., Akron, Ohio, USA). The components in panel A are put into place in the pockets (panel B), and the polymer resin poured. Modeling

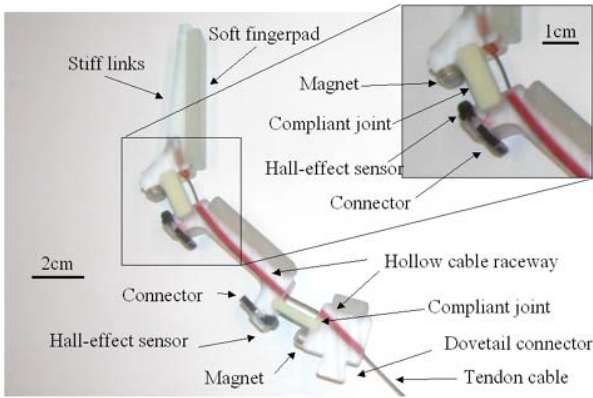


Fig. 3 Details of finger parts and placement of components.

clay is used to dam any areas to be blocked from the resin. After the layer cures, a second group of pockets is machined (both into the support wax and the stiff resin) and dammed (panel C). The polymer resins for the compliant finger joints (white) and soft fingerpads (clear) are then poured (panel D) and allowed to cure. The block is then faced off to level the surface and remove surface flaws (panel E), and the completed fingers removed from the wax support material. The entire process takes approximately 30 hours to complete, only 4 of which require human intervention.

The polymers used are two-part industrial polyurethanes. Different compositions are used for the soft fingerpads, compliant joints, and stiff links (IE35A, IE90A, and IE72DC, respectively, Innovative Polymers, St. Johns, Michigan, USA). Table I shows material properties as provided by the manufacturer.

Fig. 3 diagrams the parts of the SDM finger. The concave side of each link contains a soft fingerpad to maximize friction and increase grasp stability. The thin sections between links are the compliant joint flexures, with stiffnesses of 0.0421 Nm/rad and 0.224 Nm/rad for the proximal and distal joints, respectively. For actuation, each finger has a pre-stretched, nylon-coated stainless steel cable anchored into the distal link. This cable runs through the bodies of the proximal and base links through low-friction tubing. Due to the joint compliance the finger can be under-actuated, allowing for one tendon cable to drive both joints. A dovetail protrusion on the base link allows the finger to be securely connected to the grasper base.

### III. SENSORS

#### A. Joint Angle Sensor

Joint angle sensing in the robot fingers described above is accomplished by embedding a low output impedance linear hall-effect sensor (A3517SUA, Allegro MicroSystems, Inc., Worcester, Massachusetts, USA) on one side of the joint, and a rare-earth magnet (6.35mm diam x 3.18mm, NdFeB, 10,800 Gauss strength, K&D Magnetics, Inc., Boca Raton, Florida, USA) on the other

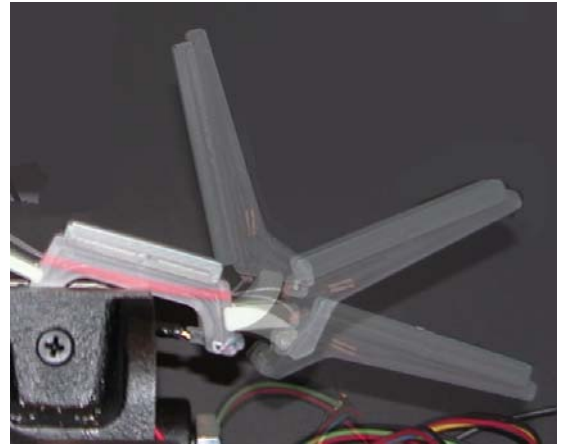


Fig. 4 Superimposed photograph of joint deflection and link motion for three positions across the travel range of the distal joint of the fingers. The center image is the rest position.

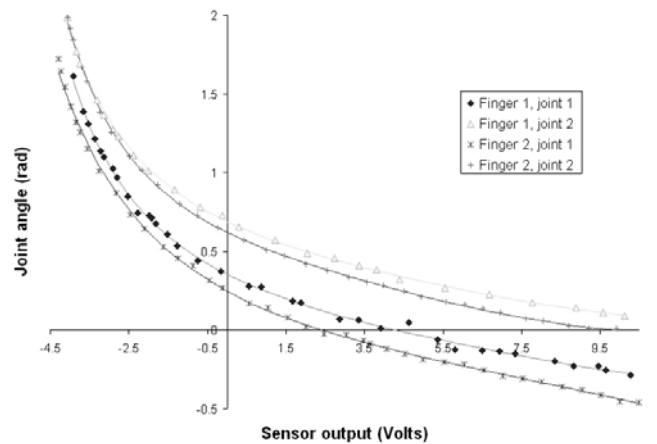


Fig. 5 Joint angle sensor calibration data and fits

side (Fig. 3 inset). Joint motion changes the distance between the two, varying the sensor output. The sensors are wired to exposed connectors (2.5mm PC board header) for connection to external cables.

Fig. 4 shows the behavior of the finger joints through their range of motion. Note that the center of rotation varies slightly with joint angle. Fig. 5 shows the output of the joint angle sensors (after amplification) and their fits versus joint deflection,  $\theta$ , for the two fingers used in this study. The fit curves are of the form

$$\theta = (c_4 V^4 + c_3 V^3 + c_2 V^2 + c_1 V + c_0)^{-1} - 1, \quad (1)$$

where  $c_i$  are the fit coefficients and  $\theta$  and  $V$  have units of (radians, volts), respectively. These sensors give sufficient sensitivity across the entire range of motion of the joints to allow for use in the control of the grasper. The RMS sensor noise was found to be approximately 40 mV.

Note that the sensor gives better resolution as the finger opens ( $\theta$  decreases) in order to optimize sensitivity during passive contact under. This enhances performance of the grasper when used as a “feeler”. More about the usage and performance of the grasper can be found in [9].



Fig. 6 Metal film strain gages embedded in beam with side-exit wires (top) and axial-exit wires.

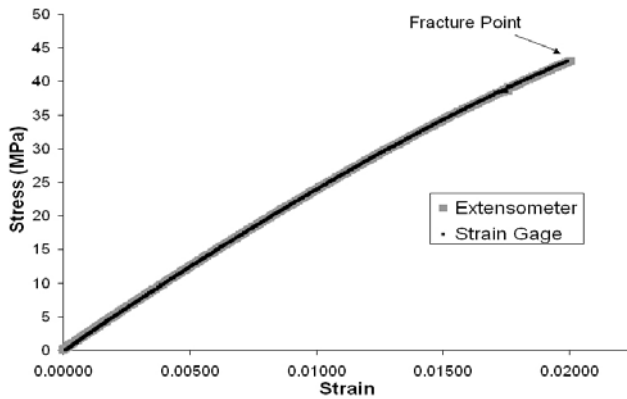


Fig. 7 Measured and actual strain in side-exit beam.

### B. Strain Gage Force Sensor

Strain gages are often used as the basis of high quality force transducers due to their high sensitivity. The drawback of strain gages is that the bonding procedure is complicated and time consuming. Integrating SDM with strain gages allows devices to be created with the high durability and ease of construction of SDM combined with the sensitivity of strain gages.

To determine the strain measuring capabilities of a strain gage embedded in a pourable plastic (IE72DC, Innovative Polymers, St. Johns, Michigan, USA), we embedded a full-bridge metal film strain gage (N2A-13-S056R-350, Vishay Micro-Measurements, Wendell, North Carolina, USA) in a beam (8.5 cm length, 1.27 cm x 0.64 cm cross-section). The beam was then loaded in tension (Series 900 Universal Test Machine, Applied Test Systems, Butler, PA, USA) and its strain at different loads was measured using a calibrated extensometer (model 2630-005, Applied Test Systems). Two types of beams were tested to examine the effects of wire placement; one with the strain gage wire leads exiting from the side of the beam, the other with wires running the axis of beam (Fig. 6).

The stress strain curve of the beam with side-exit wires is shown in Figure 7. The measured strain from the gage matches the actual strain to less than 1 percent over the entire load. No significant difference was found between the side-exit or axial-exit beam in terms of strain measuring capability. A final observation is that the output of the strain gage matched the measured strain all the way to the ultimate failure of the specimens at 2% strain,

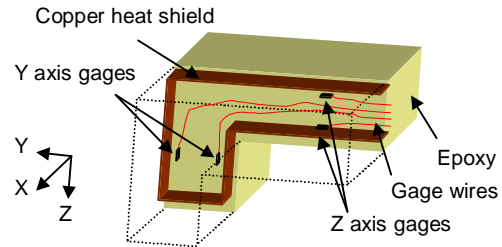
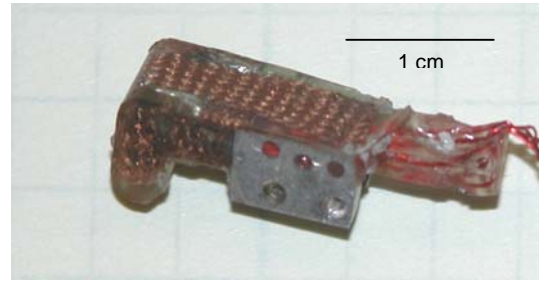


Fig. 8 Picture and diagram of three-axis force sensor. Note presence of copper heat shield.

showing the gage is well integrated into the material.

### Three-axis force sensor

Based on the success of the previous proof of concept, and the relative ease of embedding strain gages versus bonding, we integrated six strain gages to create a miniature gripper (5 mm x 6.5 mm x 14.5 mm) with an embedded three-axis force sensor. Using the SDM approach, robust, high quality force sensors can be built for relatively little cost because the time consuming bonding process is avoided.

Our force sensor is a dual beam configuration. One strain gage is located on each of the four sides of the proximal bending beam, sensing two bending moments (corresponding to X and Z forces). Two final strain gages are located in the distal bending beam to sense the final axis (Y) of force. The sensor is integrated with an aluminum base allowing simple attachment to manipulators. Because of the SDM process, wires to the individual gages are integrated into the sensor core, removing the need for strain relief. A further advantage is that all wires leave the sensor at the same point providing straightforward and robust wire management.

The sensor construction is carried out in a two pour casting process. The first pour embeds the strain gages and wires in an epoxy core and attaches the core to the aluminum base. The second pour embeds a copper braid (Ungar-Wick #4, Ungar Products, Apex, North Carolina, USA) heat shield around the core. The epoxy used (Resin 105 Fast Cure, West System, Bay City, Michigan, USA) was chosen for its stiffness and low creep properties. Silicon strain gages (SS-037-022-500P, Micron Instruments, Simi Valley, California, USA) were used to achieve high sensitivity in a small package.

Fig. 9 shows the calibrated response to a Z-axis (worst case axis) load for each sensor axis, with a maximum deviation from linear of 17%. The force sensor has greater

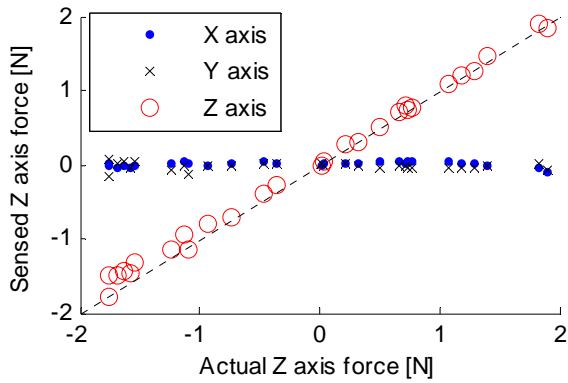


Fig. 9 Sensor response to Z-axis (worst case) loads showing linearity

than a 2 N range with a maximum RMS noise on each axis of 0.09 N. Fig. 11 shows the force tracking ability of the sensor in the Y-axis, demonstrating good correspondence with the actual force and little off-axis crosstalk.

Strain gage based sensors built using SDM are especially sensitive to output fluctuations due to temperature variation. Because SDM material is an insulator, temperature gradients can easily exist in the material, causing a temperature difference between strain gages located at opposite sides of a bending beam. This difference in temperature causes a signal that is indistinguishable from strain. For larger sensors, one can use multiple gages on the same backing to compensate for temperature. To achieve the small size of our sensor, we used only two strain gages per axis of force and incorporated a heat shield made of copper braiding to equalize the temperature between gages. Use of the heat shield was critical to an effective sensor; earlier designs with the same size and no heat shield experienced measured drift of 1.2 N over 5 minutes in open air. The sensor with the heat shield drifts only 0.15 N in 5 minutes (Fig. 10) - almost an order of magnitude improvement.

### C. Tactile Sensor

A tactile sensor has been developed for integration with the soft fingerpads (Fig. 11). An array of these sensors can be used to sense a two-dimensional pressure distribution across the fingerpad. The sensor uses a reflective object sensor (OPB608R, 660 nm emitter wavelength, Optek Technology, Carrolton, TX, USA) that consists of an LED and photodetector. As the finger applies force to an object, the pad deforms inwards, bringing the reflective inner surface of the fingerpad closer to the embedded sensor and causing a change in detector current. The slanted struts reduce stiffness in the normal contact direction. As shown in Fig. 11, black and white dyes were used in the support and pad materials (IE72DC and IE20AH – see Table I for material properties) to shield the sensor from ambient visible light and increase reflectance. The sides of the sensor can also be easily enclosed.

The stiffness of the pad is very low - on the order of 1

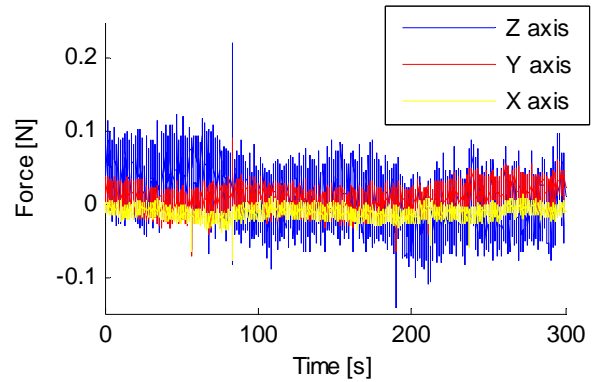


Fig. 10 Noise in each axis of the sensor in Newtons over 5 minutes at 50 Hz sample rate

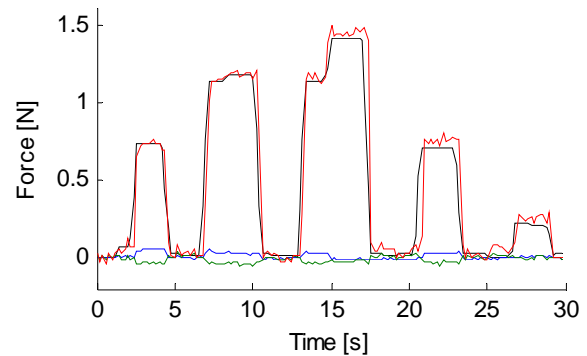


Fig. 11 Sensor response to Y axis loads

kN/m, depending on contact location and geometry. Fig. 12 shows the sensor output as a function of applied force for the various indenter diameters. It is clear from the figure that contact geometry plays a role in sensor output. This effect is due to both the difference in effective stiffness and the curvature of the reflective surface, which can deform with small objects to deflect light away from the detector. Note the higher sensitivity to smaller loads, a property useful in contact detection.

Although this prototype contains only one optical sensor, multiple sensors can be embedded in the pad at about one every fifteen millimeters under the current design. Combining an array of the tactile sensors into a fingerpad will yield an inexpensive, compliant, distributed pressure sensor that can sense contact location on the fingerpad, as well as determine object geometry based on contact location. The array density, or contact position resolution, is limited only by the size of the emitter/detector package.

### D. Piezofilm Contact Sensor

We have integrated a piezoelectric polymer film element (model LDTO-028K, MSI sensors, Hampton, VA, USA) into a compliant pad to make a robust, low-threshold contact sensor (Fig. 14). These sensors generate an electrical charge in proportion to the applied strain, have excellent frequency sensitivity, but no static response. By embedding the flexible sensor just under the contact

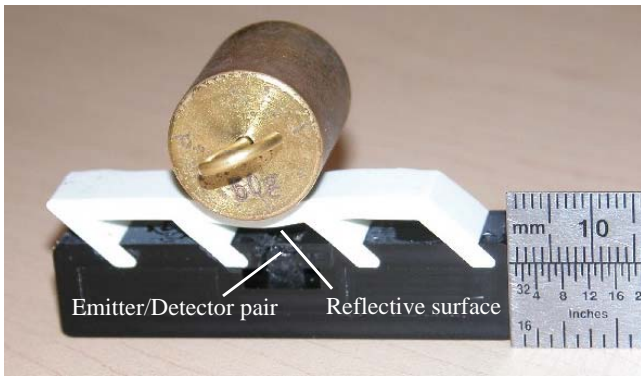


Fig. 12. Tactile sensor prototype with 50g weight placed over the sensor. The angled strut flexures separate the reflective surface from the sensor face. Note the curvature of the reflective surface due to the applied load.

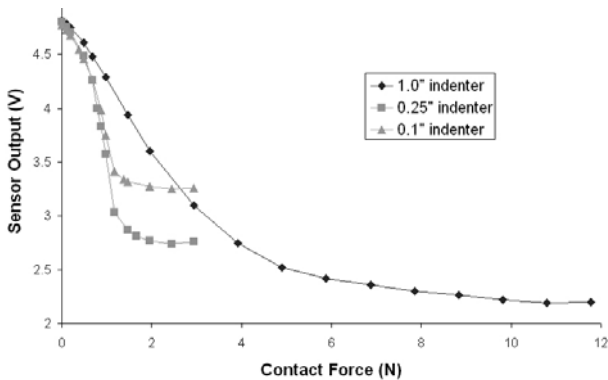


Fig. 13 Optical sensor output vs. contact force for various spherical indenter geometries

surface, we sense the transient when the fingerpad is deformed on initial contact.

To test the resolution of the sensor to a short contact, a load of 0.03 N was quickly removed from the sensor in less than 10 ms. This stimulus produced a 200 mV peak response, approximately 5 times the RMS sensor noise (40 mV). The sensor can therefore quickly respond to low force contact transients. This allows a manipulator to react quickly to minimize contact forces with the environment, yet still operate at a reasonable speed.

Similar sensors have been developed for contact and transient detection, as well as perception of small shapes and incipient slips [11]. The sensor was fabricated as a separate device and then assembled with the robot finger. While this provided good sensitivity, the need for assembly increased the complexity of the fabrication process and reduced the durability of the resulting gripper in comparison to the present SDM approach.

#### IV. CONCLUSIONS AND FUTURE WORK

Shape Deposition Manufacturing (SDM) has shown great promise in enabling biomimetic construction of robust robots that part from traditional design methods. The capability to create spatially-varying materials for complex flexures and the added durability from embedded components will surely prove appealing to researchers



Fig. 14. Piezofilm contact sensor.

frustrated with the fragility and complexity of robots built with traditional manufacturing methods. To further the usefulness of SDM, we have developed sensors for use with the process that cover four of the most utilized sensor types in robotics – joint angle, force, taction, and contact.

To continue the development and evaluation of these sensors, our next step is to create a more sensorized robotic hand by implementing combinations of sensors in an SDM grasper. The performance of these hands will be evaluated across a large range of grasping tasks, with particular attention to the information that can be gleaned from the different sensor suites. This analysis should speak not only to the sensors' effectiveness, but also to the nature of the information needed to complete the various grasping tasks.

#### ACKNOWLEDGMENT

The authors would like to thank Mark Cutkosky, Moto Hatanaka, and Miguel Piedrahita for their advice and assistance with implementing the SDM process. Also, we would like to thank Chris Johnson for his assistance in implementing the process, and Francisco Isenberg for his work on the construction many of the sensor prototypes.

#### REFERENCES

- [1] J. E. Clark et al., "Biomimetic design and fabrication of a hexapedal running robot," Proceedings of the 2001 International Conference on Robotics and Automation, Seoul, Korea, 2001.
- [2] A. M. Dollar, "Arthropod Grasping and Manipulation: A Literature Review," Harvard BioRobotics Laboratory Technical Report, 2001.
- [3] R. Merz, F. B. Prinz, K. Ramaswami, M. Terk, L. Weiss, "Shape Deposition Manufacturing," Proceedings of the Solid Freeform Fabrication Symposium, Univ. of Texas at Austin, Aug. 8-10, 1994.
- [4] iRobot Corporation, Government and Industrial Robotics Division, Burlington, MA, USA, (www.irobot.com).
- [5] D. F. Hougen et al., "A Miniature Robotic System for Reconnaissance and Surveillance," Proc. of the 2000 IEEE Intl. Conf. on Robotics and Automation, San Francisco, CA, April 2000.
- [6] D. A. Theobald et al., "Autonomous Rock Acquisition," Proceedings of the AIAA Forum on Advanced Developments in Space Robotics, Madison, Wisconsin, August, 1-2, 1996.
- [7] A. T. Asbeck et al., "Scaling Hard Vertical Surfaces with Compliant Microspine Arrays," Proceedings of Robotics: Science and Systems, Cambridge, MA, 2005.
- [8] C. Stefanini, M. R. Cutkosky, P. Dario, "A high force miniature gripper fabricated via shape deposition manufacturing," Proc. of the 2003 Intl. Conf. on Robotics and Automation, Taipei, Taiwan, 2003.
- [9] A. M. Dollar and R. D. Howe, "Design and Evaluation of a Robust Compliant Grasper using Shape Deposition Manufacturing," Proceedings of the 2005 ASME International Mechanical Engineering Congress and Exposition, 2005.
- [10] A. M. Dollar and R. D. Howe, "Towards grasping in unstructured environments: Grasper compliance and configuration optimization," Advanced Robotics, vol. 19(5), pp. 523-544, 2005.
- [11] R. D. Howe and M. R. Cutkosky, "Dynamic tactile sensing: Perception of fine surface features with stress rate sensing," IEEE Trans. on Robotics and Automation 9(2):140-151, April 1993.